

Largely Enhanced Efficiency in ZnO Nanowire/p-Polymer Hybridized Inorganic/Organic Ultraviolet Light-Emitting Diode by Piezo-Phototronic Effect

Qing Yang,^{†,‡,||} Ying Liu,^{†,||} Caofeng Pan,[†] Jun Chen,[†] Xiaonan Wen,[†] and Zhong Lin Wang^{*,†,§}

[†]School of Material Science and Engineering, Georgia Institute of Technology, Atlanta, Georgia 30332-0245, United States

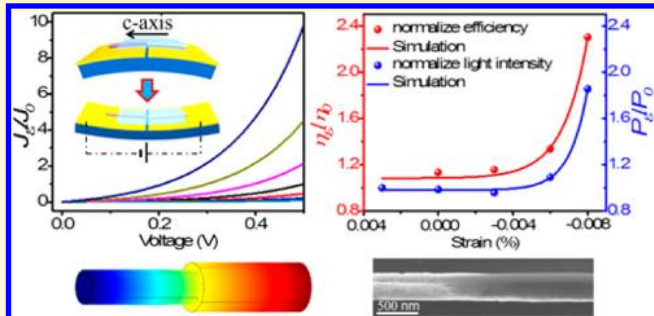
[‡]Key Laboratory of Modern Optical Instrumentation, Department of Optical Engineering, Zhejiang University, Hangzhou 310027, China

[§]Beijing Institute of Nanoenergy and Nanosystems, Chinese Academy of Sciences, China

Supporting Information

ABSTRACT: ZnO nanowire inorganic/organic hybrid ultraviolet (UV) light-emitting diodes (LEDs) have attracted considerable attention as they not only combine the high flexibility of polymers with the structural and chemical stability of inorganic nanostructures but also have a higher light extraction efficiency than thin film structures. However, up to date, the external quantum efficiency of UV LED based on ZnO nanostructures has been limited by a lack of efficient methods to achieve a balance between electron contributed current and hole contributed current that reduces the nonradiative recombination at interface. Here we demonstrate that the piezo-phototronic effect can largely enhance the efficiency of a hybridized inorganic/organic LED made of a ZnO nanowire/p-polymer structure, by trimming the electron current to match the hole current and increasing the localized hole density near the interface through a carrier channel created by piezoelectric polarization charges on the ZnO side. The external efficiency of the hybrid LED was enhanced by at least a factor of 2 after applying a proper strain, reaching 5.92%. This study offers a new concept for increasing organic LED efficiency and has a great potential for a wide variety of high-performance flexible optoelectronic devices.

KEYWORDS: ZnO, nanowire, hybrid LED, piezo-phototronic effect



ZnO nanowires (NWs) have become a subject of great scientific and technological interest because of their unique semiconductor, photonic, and piezoelectric properties for a range of applications in photonics, electronics, sensors, and energy harvesting.^{1–5} With a direct band gap of about 3.30 eV, a large excitonic binding energy about 60 meV, and a large refractive index, ZnO NWs are among the most promising materials for the next generation optoelectronic devices operating in ultraviolet (UV) region, such as light-emitting diodes (LEDs),^{6–10} photodetectors,^{11,12} and solar cells.^{13,14} Nanoscale hybrid materials containing organic as well as inorganic components have attracted considerable attention in recent years, as they promise new properties that may not easily be available from conventional materials. For example, the hybrid structure devices can combine the high flexibility of polymers with the structural and chemical stability of inorganic nanostructures, compatible with low cost, polymer printing techniques.^{15,16} To date, inorganic/organic hybrid LEDs with n-type ZnO nanostructures have been realized in many different systems, including poly(3,4-ethylenedioxythiophene):polystyrenesulfonate (PEDOT:PSS),^{17,18} p-type N,N'-diphenyl-N,N'-bis(1-naphthyl)-1,1'-biphenyl-4,4'=diamine (α -

NPD),¹⁹ N,N'-di(naphth-2-yl)-N,N'-diphenyl-benzidine (NPB),²⁰ poly(N-vinylcarbazole) (PVK),²¹ poly[2-methoxy-5-(2-ethylhexyloxy)-1,4-phenylenevinylene] (MEH-PPV),²² and poly(3-methylthiophene) (PMT),²³ and so forth. However, organic/inorganic hybridized UV LEDs based on ZnO nanostructures have shown very low external quantum efficiencies (EQEs) due to the difficulties in achieving current balance between electrons and holes and high nonradiative recombination induced by surface defects.^{18,20,22–24} In most of the reports, there were no data about conversion efficiency or EQE of ZnO NW/organic hybrid LED.

The EQE of LEDs, which is the photons emitted per electron injected, depends on the balance of the currents and therefore on the charge injection rates at the cathode and anode interfaces. If one sign of carrier dominates over the other, most of the majority carriers across from one electrode to the other do not experience recombination, which contributes to the current instead of photon emission. Therefore, it becomes

Received: November 10, 2012

Revised: January 14, 2013

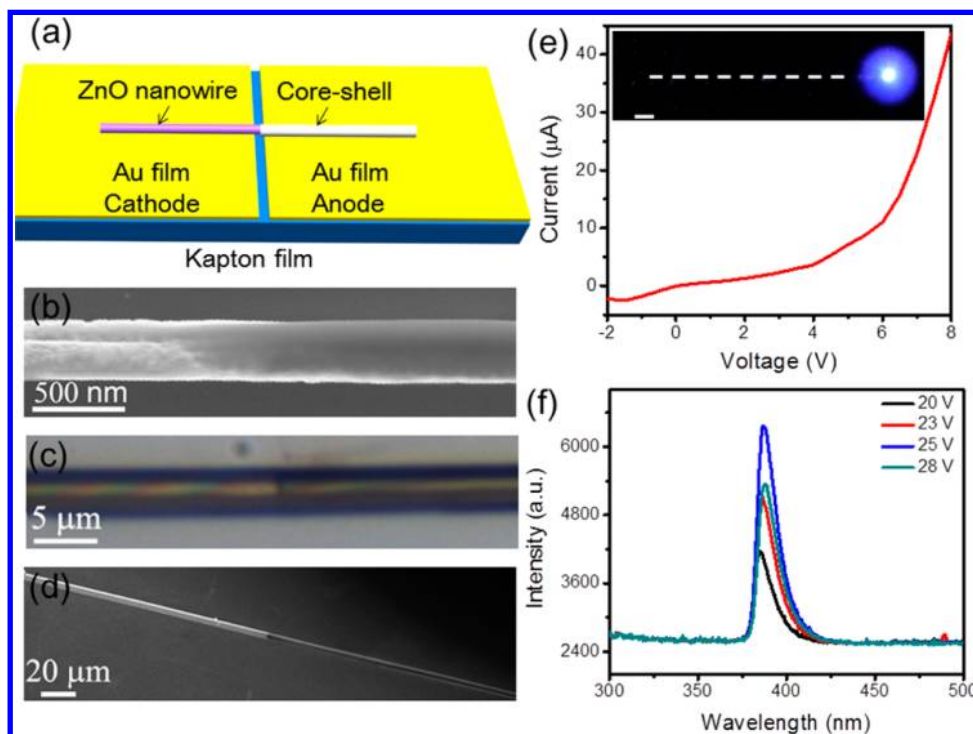


Figure 1. Characterization of ZnO NW/p-polymer core–shell UV LED. (a) Schematic diagram of device structure. (b) SEM image of a ZnO NW/PEDOT:PSS core shell structure. (c, d) OM and SEM image of a ZnO microwire/PEDOT:PSS core–shell structure. (e) I – V curve of the LED, the inset is a CCD image of the LED at 25 V biasing voltage, and the dashed line represents the physical location of the ZnO NW/p-polymer core–shell structure, scale bar 10 μm . (f) EL spectrum as a function of the forward biased voltage.

critical to achieve the best possible current balance in the fabrication of LEDs such as using suitable electrode materials,²⁵ insulator as carrier blocking layers,²⁴ and post-treatment of organic materials.²⁶ In our previous work, we have already shown that piezo-phototronic effect can enhance the external efficiency of an inorganic LED fabricated using a single ZnO micro/nanowire on a GaN substrate.²⁷

Here we demonstrate how the Schottky contact and piezo-phototronic effect can be effectively utilized to enhance the external efficiency of an inorganic/organic LED using a single ZnO nanowire/p-polymer core–shell structure. The emission light intensity and EQE has been enhanced to 190% and 230% after applying a -0.008% compressive strain when the *c*-axis of ZnO nanowire is pointing away from the p-polymer. Meanwhile, when the *c*-axis of ZnO nanowire is pointing toward the p-polymer, the emission light intensity and EQE has been enhanced to 230% and 370% after applying a 0.017% tensile strain. The asymmetric change in current under forward and reverse bias indicates that the performance enhancement is attributed to the piezo-phototronic effect. This work not only proves that the applications of the piezo-phototronic effect can extend from rigid inorganic to flexible organic materials but also offers a more compact and lower cost device structure as well as a very simple fabrication process for high efficient hybrid UV LED. Numerical simulations fit well to the experimental results, and the physical mechanism is proposed with considering the big difference of organic materials and inorganic materials.

Our experiments were carried out based on the following design. ZnO nanowires were synthesized using a high-temperature thermal evaporation process.²⁸ The device structure is schematically shown in Figure 1a. Using a 3D micromanipulation stage under an optical microscope, a single ZnO NW was picked up from the substrates, and the free end

was dipped in a small PEDOT:PSS droplet to form a ZnO NW/p-polymer core–shell structure. Scanning electron microscopy (SEM) images (Figure 1b and d) show that a thin and smooth PEDOT:PSS film (about 10 nm) is coated on ZnO NW uniformly, indicating an excellent contact and good interface forming between these two materials, which is simply called a core–shell structure for description purpose. A Kapton (polyimide) film ($20 \text{ mm} \times 8 \text{ mm} \times 0.5 \text{ mm}$) covered by Ni/Au ($20/50 \text{ nm}$) film or ITO film electrodes with a well-controlled gap was used as the substrate. The ZnO NW/p-polymer core–shell nanostructure was placed across the gap with a close contact with electrode film. To avoid short circuit, the shell should be terminated inter the gap of two Au electrodes, as shown in Figure S1b of the Supporting Information. A transparent polystyrene (PS) tape was used to cover and fix the nanowire. The experimental setup is shown schematically in Figure S1. A 3D stage was used to fix the device, and another 3D stage was used to introduce strain. The Kapton substrate was bent concave up and convex down under different forces. Considering the relative size of the wire and the substrate, compressive or tensile strain was introduced mainly axially depending on the bending direction of the substrate. The strain was quantified by the maximum deflection of the free end of the substrate.²⁹

The I – V characteristics and dependence of the emission intensity on applied voltage of an as-fabricated LED without applying additional strain are presented in Figure 1e and f. A strong UV emission peak is obviously observed while visible broad-band luminescence also exists in some devices. The UV emission is centered at a wavelength of 387 nm and has a full width at half-maximum (fwhm) of 13 nm, ascribed to bound-exciton or vacancy-related transitions in ZnO NWs.^{30,31} The EQE and power conversion efficiency of an as-fabricated single

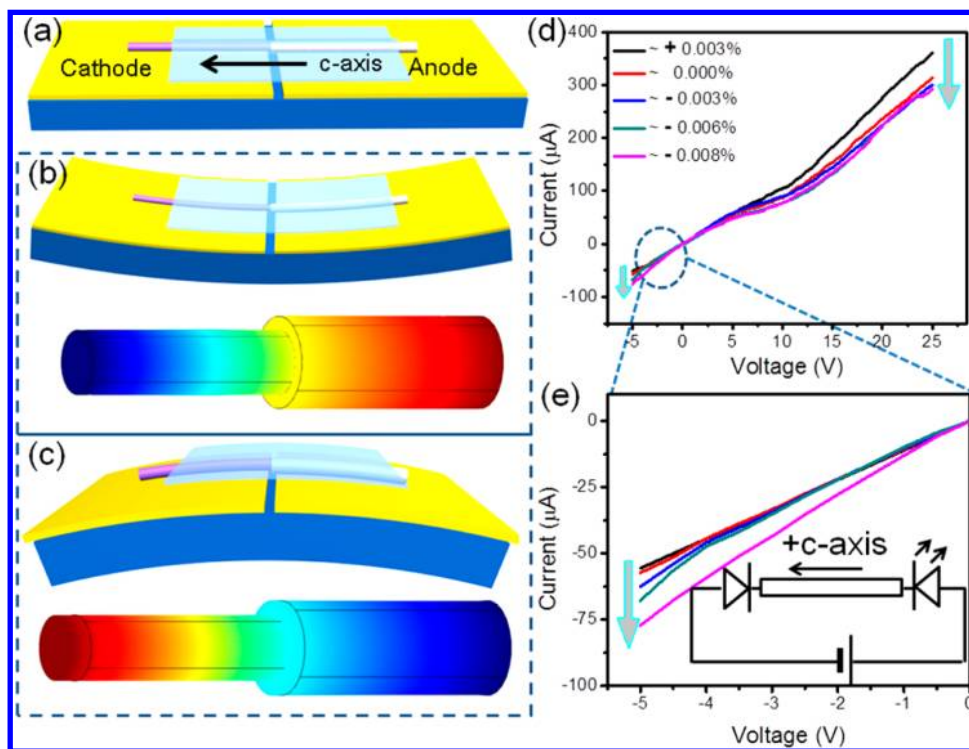


Figure 2. Electric characteristics of a ZnO NW/p-polymer core–shell UV LED with *c*-axis pointing away from p-polymer under different strain. (a) Schematic diagram of the device. (b) Simulated piezopotential distributions in the ZnO NW under compressive strain. (c) Simulated piezopotential distributions in the ZnO NW under tensile strain. The diameter and length used for calculation are 1 μm and 10 μm , respectively. The compressive and tensile strain are about -2% and 2% , respectively. The conductivity of the ZnO is ignored in the simulation for simplicity. (d) *I*–*V* characteristics of the device at forward bias with the variation of the applied strain. (e) The enlarged picture of *I*–*V* curve circled by dashed line. Insets are the configuration of the device and direction of forward bias.

ZnO nanowire inorganic/organic core–shell LED before applying strain was measured to be about 1.6% and 0.5%, respectively. It is found that the relative high efficiency benefits from the core–shell structure and the Au electrodes (Figure S2 and Table S1). Among the three device structures in Figure S2, the hybrid structure LED based on nanoscale core–shell structure with Au electrodes has the highest EQE, followed by the core–shell structure with ITO electrodes; the hybrid structure based on ZnO NW and ITO film shows the lowest efficiency. Compared with the conventional hybrid structure LED based on ZnO NW and spun-coating PEDOT:PSS film, the hybrid structure LED based on nanoscale core–shell structure could offer better contact and a more uniform interface (Figure 1b–d), which is good for achieving high efficiency LED. Furthermore, defects on ZnO NW surface may be passivated by a p-polymer, resulting in a decrease of the nonradiation recombination and increasing in light output.

An important factor influencing the conversion efficiency of LED is the current balance including charge injection rate and carrier mobility of electrons and holes. In our device, electrons are the majority carrier, and recombination is limited by hole injection because of the large barrier height for hole transport. As shown in Figure S3, there is a 0.6 eV barrier for electron injection from Au into ZnO's conduction band and a 1.0 eV barrier between the ZnO conduction band and the PEDOT LUMO (lowest unoccupied molecular orbit). The hole injection barrier is 0.1 eV between the Au and PEDOT:PSS HOMO (highest occupied molecular orbit) and 2.7 eV for electron injection from PEDOT:PSS HOMO into ZnO valence band. Thus the total barriers for electrons and holes when using Au as electrodes are 1.6 eV and 2.8 eV, respectively. As a

comparison, if using ITO as electrodes, the total barriers for electrons and holes are 1.0 eV and 3.2 eV, respectively. Compared with ITO electrodes, Au electrodes will balance the electron current and hole current more easily by increasing the barrier for electron transport and reducing that for holes simultaneously. The results are similar to that utilizing a thin oxide layer as carrier blocking layer to improve the performance of organic LED.²⁴ Our experiment results are consistent with the above analysis. In Table S1, we can see that the external efficiency of our ZnO NW/p-polymer core shell structure is about 1.6% and 0.3% for structure using Au electrodes and ITO electrodes, respectively.

Furthermore, in the next step of our work, we show that piezoelectricity can significantly enhance the EQE, which is a complete new approach to improve the performance of inorganic/organic hybrid LED. As shown in Figures 2 and 4a, under a fixed forward bias above the turn-on threshold voltage, the current decreases step-by-step when a variable strain is applied from 0.003% tensile strain to -0.008% compressive strain. An important characteristic of the current change is the asymmetric change of *I*–*V* curve at negative and positive bias (Figure 2d and e): while the current under forward bias decreases with applied strain, under reverse bias the current increases. It indicates that the change is mainly due to genuine piezo-phototronic effect that is from the polarized piezopotential.³² Other factors induced by external strain such as piezoresistance, band shifting, or contact area change will induce symmetric change at both ends of the nanowire regardless the polarity of the applied voltage.^{27,32}

Importantly, from experimental results shown in Figure 1, the light emission should be localized near the end surface of

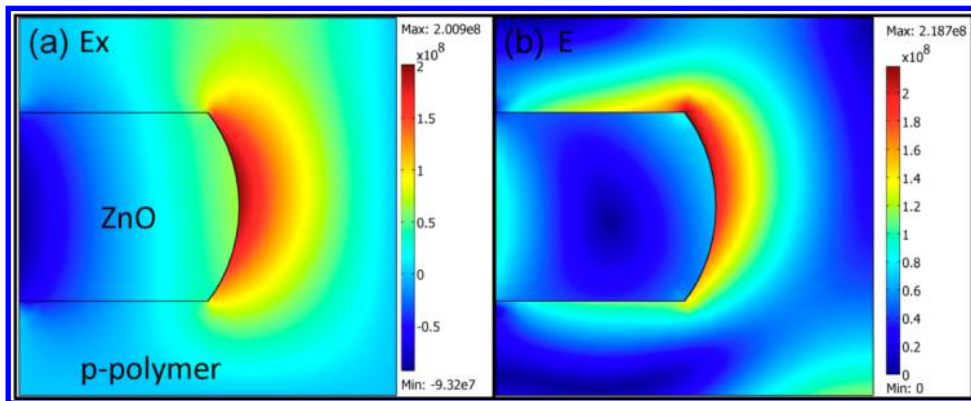


Figure 3. Simulated distribution of electric field in the contact of ZnO nanowire and PEDOT:PSS. (a) Electric field along the axial direction of the nanowire and (b) the magnitude of the total electric field E . Simulation details are sketched in the Supporting Information.

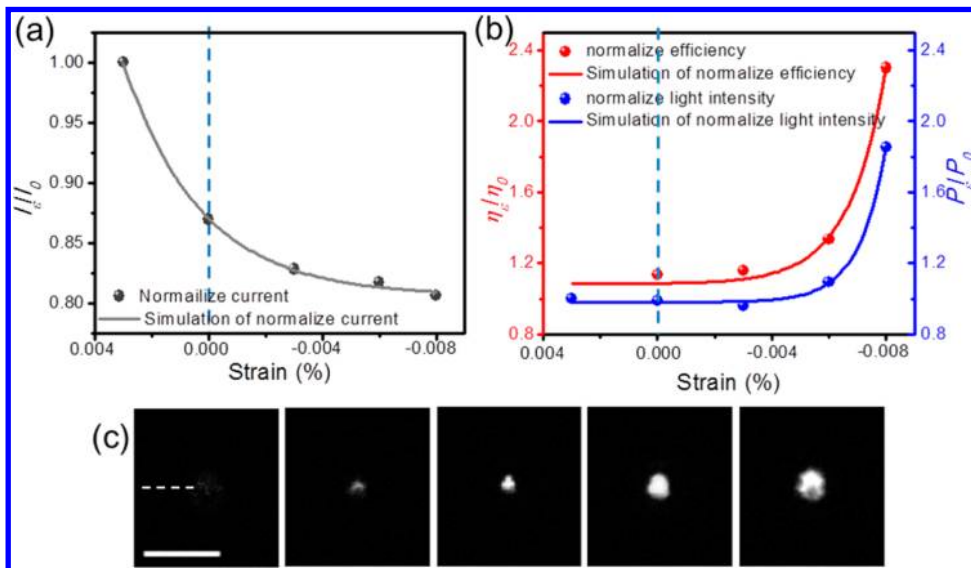


Figure 4. Enhancement of emission light intensity and conversion efficiency of a ZnO NW/p-polymer core–shell UV LED with c -axis pointing away from p-polymer under different strain at 25 V biasing voltage. (a) Change in relative injection current I_e/I_0 under different strain. (b) Change in relative light intensity P_e/P_0 and external efficiency η_e/η_0 under different strain. (c) CCD images recorded from the emitting end of a packaged single wire LED under different applied strain; the dashed line represents the position of ZnO NW/p-polymer core–shell structure, scale bar 10 μm .

the nanowire, where ZnO is in contact with PEDOT:PSS. To verify this observation, we have carried out a numerical simulation about the distribution of electric field near the ZnO/p-polymer interface, and the results are shown in Figure 3. According to this simulation, most of the electric field is localized in the x -direction (the axial direction of the nanowire) near the end polar surface of the nanowire where ZnO is in contact with PEDOT:PSS, which is also the area where piezoelectric charges are distributed. Thus, the influence of piezo-phototronic effect is significant to the light emission. Our following analysis is based on the light emission at the end polar surface of the nanowire instead of the side surface. The change of the current with strain can be determined by²⁹

$$\ln\left(\frac{I_e}{I_0}\right) = \Delta\Psi/kT \quad (1)$$

Since piezopotential has a linear relationship with the external strain, we can expect that the change of current (I_e/I_0) has an exponential relationship with the external strain, as shown in Figure 4a.

Surprisingly, in the experiments, the light emission intensity is increased step-by-step while the forward current is decreased gradually (Figure 4b) when we apply a compressive strain. The light output enhancement can be directly observed in optical images recorded by a CCD. The change of the light intensity increases exponentially with the increased compressive strain (Figure 4b). The ocular sensitivity of the human eye is very low at the ultraviolet wavelength, and the silicon diode used to measure luminance is not sensitive at 380 nm either. Thus the normally used luminous efficiencies in terms of Cd/A or lm/W are not good measures of UV LED. Better measures of the performance are the EQE and overall emission efficiency (also called power-conversion efficiency). The overall emission efficiency η is defined as the ratio of the emitted optical power P to the applied electrical power,

$$\eta = \frac{P}{I \times V} = \eta_{\text{ex}} \frac{h\nu}{eV} \quad (2)$$

where P is the emitted optical power, I is the current, V is the applied voltage, h is Planck's constant, e is elementary charge, and ν is the frequency of the emitting light. η_{ex} is the EQE, the

ratio of the externally produced photon flux to the injected electron flux,

$$\eta_{\text{ex}} = \frac{P/h\nu}{I/e} \quad (3)$$

The light intensity under -0.008% compressive strain was enhanced to 190%, while the current was decreased to 81% of the original value. The light output increase and current decrease will dramatically enhance the EQE and conversion efficiency according to eqs 2 and 3. The efficiency is enhanced to 230% after applying -0.008% compressive strain.

In our experiments, some of the devices show an opposite trend of change, which means that the light output and efficiency is enhanced under tensile strain (Figures S4 and S5). The emission light intensity and EQE have been enhanced to 230% and 370%, respectively, after applying a 0.017% tensile strain. The absolute conversion efficiency and the EQE of the LED are 1.85% and 5.92%, respectively, after applying a tensile strain, which is comparable to that of inorganic pn junction LED and quantum-well enhanced nanowire LED.³³ The opposite change in two different types of NWs is attributed to the switching in signs/polarity of the piezopotential, which depends on the orientation of the *c*-axis of the ZnO wire. Statistically, we have 50% chance in experiments to have the ZnO wire oriented along the *c* or $-c$ direction (the axial direction of the wires). It is noted that, in two different kinds of devices, the *I*–*V* curve change is both asymmetric for negative and positive bias, which is one of the judging criteria for the piezo-phototronic effect.³² In experiments, the LED operation voltage is randomly chosen (above the turn-on threshold voltage), and the enhancement is calculated at the chosen applied voltages. We found that the enhanced effect has no dependence on applied voltage from testing on more than 10 devices. This indicates that the enhancement occurs across a range where the forward bias is larger than the turn-on threshold voltage, which can also be observed from the similar trend of current change at different voltages after applying strain.

The gigantic efficiency enhancement by the piezo-phototronic effect in ZnO nanowire/p-polymer core–shell structure LED can be explained schematically in Figure 5. The schematic band diagram of the device without strain shows that the barrier for hole injection from PEDOT:PSS into ZnO is approximately 3 eV (Figure S3b). Therefore, the extremely high barrier height for holes injection makes the recombination being largely limited by hole injection and transport. The efficiency is low as

majority electrons flow through without sufficient recombination with holes. When the device is applied with proper strain under forward bias, a distinctive change will be induced on the band diagram due to the piezoelectric effect, which is proved to enhance the electron–hole recombination and efficiency significantly. Numerical simulation of the piezopotential distribution on the ZnO NW/p-polymer core–shell structure shows that a negative potential drop is created along $+c$ axis of ZnO NW when the NW is under *c*-axis compressive strain, while an oppositely distributed piezopotential is created when the NW is under *c*-axis tensile strain, assuming that ZnO NW is intrinsic or low-doping. If the *c*-axis of the ZnO NW is pointing away from the p-polymer and the ZnO NW under *c*-axis compressive strain, the effect of the local negative piezopotential at the cathode will increase the Schottky barrier height, while the local positive piezopotential near the p–n junction (at the end of ZnO NW where light is illuminated as shown in Figure 1) will introduce a carrier channel owing to a dip at the local band, with considering the narrow distribution width of the piezoelectric polarization charges. The formation of the dip can be derived from the coupling of Poisson equation and piezoelectric constitutive equation.²⁷ A theoretical analysis of current distribution shows that the current mainly flows through the adjacent of the illuminating end face of NW. Thus overlapping of localized piezo-charges and current density can enhance the piezo-phototronic effect and light output of LED significantly.

The polarity of the bias applied on the entire LED device is defined in reference to the p–n junction. If the device is forward-biased, the Schottky contact between the Au-ZnO is under reverse bias, which largely dictates the transported current. An increase in barrier height will result in a decrease in electron current. The increase of light output occurs with the decrease of the forward current may be suggested from the carrier trapping channel near the interface caused by the existence of piezo-charges. Electrons and holes can be temporarily trapped and accumulated in the channel and its adjacent. Since abundant electrons are available in ZnO and the extreme high barrier height for holes, the efficiency of the hybrid LED is largely dominated by the local concentration of holes. The trapped holes can increase the hole injection from PEDOT:PSS into n-ZnO, which increases the recombination efficiency of electrons and holes near the junction, leading to a large increase in emission intensity and enhancement of efficiency. On the other hand, if the *c*-axis of ZnO is pointing to the p-polymer, a tensile strain will introduce the same sign piezo-charges at the Schottky contact and p–n junction region as that introduced by the compressive strain on an opposite *c*-axis orientation of the NW. In our experiments, we found that, statistically, the light output and efficiency of about 50% of the devices are enhanced under compressive strain (Figures 2 and 4), while the other half were enhanced under tensile strain (Figures S4 and S5), depending on the orientations of the *c*-axis of the NWs. Furthermore, we measured the light intensity of a ZnO NW/p-polymer LED under different strain in a strain applying-releasing cycle (Figure S6). The good reproducibility in a cycle shows good stability and repeatability of our device. Another interesting phenomenon can also be observed in Figure S6. The light emission intensity gets further enhanced when we apply a compressive strain with absolute value larger than 0.008% . The slope of the curve becomes smaller when the strain absolute value is larger than 0.008% which may be caused by piezoelectric nonlinearity, elastic nonlinearity, and the

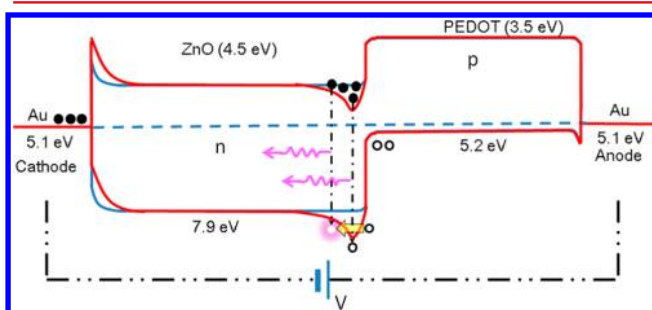


Figure 5. Proposed mechanism of the enhanced light emission under strain for a ZnO NW/p-polymer core–shell UV LED under different strains. The red line represents the band diagram considering piezo-phototronic effect, while the blue line represents the case without considering the piezo-phototronic effect.

change of electronic parameters of the core–shell structures under relative large strain, and so forth.^{34,35} In this paper, our major focus is on the effect under relative small strain for simply and clearly understanding the piezo-phototronic effect. The nonlinear piezo-phototronic effect shall be investigated in future work.

To further verify our proposed mechanism, we did numerical simulation to study the piezoelectric effect on the ZnO NW/PEDOT:PSS device. Light is emitted when the p–n junction is under forward bias, and the current of the whole device is dominated by the reverse Schottky junction. The behavior of reversely biased Schottky contact can be described by the thermionic field emission (TFE) theory considering the tunneling effect. From previous theoretical study on piezo-phototronic photodetectors, our p–n junction–Schottky junction piezo-phototronic device has a similar behavior.³²

$$I = S J_c \exp\left(\frac{q}{akT} \frac{1}{2e} \rho_{\text{piezo}} W_{\text{piezo}}^2\right) \times \left\{ \exp\left[V \frac{q}{kT} c_1 \left(1 - \frac{1}{a}\right)\right] - 1 \right\} \quad (4)$$

where I is the device current, S is the contact area, J_c is the parametrized saturated current, q is electron charge, k is the Boltzmann constant, T is temperature, ϵ is the dielectric constant, ρ_{piezo} is the density of the strain-induced piezo-charges in ZnO nanowire adjacent to the interface, W_{piezo} is the width of the piezo-charge distribution, a is the parameter for tunneling in the TFE theory, and c_1 is the proportion of voltage component applied on the reversely biased Schottky contact. For ZnO nanowires, $P = e_{33}s_{33} = \rho_{\text{piezo}}W_{\text{piezo}}$, $\epsilon = \epsilon_s\epsilon_0$, with $\epsilon_s = 8.9$. For simplified calculation, we take $c_1 = 0.8$ and $a = 1.2$. The simulated result is shown in Figure 6. The trend of change in forward current under different strain is consistent with our experimental results.

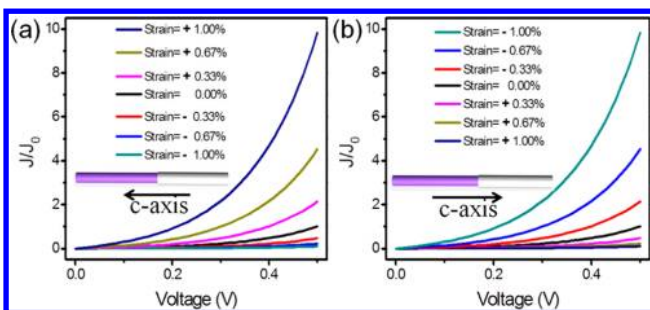


Figure 6. Results for numerical simulation of a ZnO NW/p-polymer core–shell UV LED. Simulated current–voltage characteristics under different strains with (a) c-axis point away from p-polymer and (b) c-axis pointing to p-polymer.

For the case that the device is reversely biased, the Schottky contact is forward-biased, and the p–n contact is reversely biased. When the electric field is sufficiently high at the p–n junction, a finite probability exists for interband quantum tunneling. Assuming a triangular potential barrier, the net current can be obtained by solving the Schrödinger equation, and the equation takes the form³⁶

$$J_t = \frac{q^2 \xi}{36\pi\hbar^2} \sqrt{\frac{2m^*}{E_g}} D \times \exp\left(-\frac{4\sqrt{2m^*} E_g^{3/2}}{3q\hbar\xi}\right) \quad (5)$$

where D is the integral of the energy along Fermi level, E_g is band gap, m^* is the effective electron mass, and the average electric field is given by $\xi = [(q(\psi_{\text{bi}} - V)N_A N_D)/(2e(N_A + N_D))]^{1/2}$. While the application of strain changes built-in potential ψ_{bi} , the average electric field is also changed. The channel induced by positive piezopotential will increase the built in potential. When built-in potential increases, tunneling current increases and vice versa.

Because of the polarity of the piezopotential, the asymmetric change of the I – V curve under positive and negative voltage has been theoretically proved to be the criteria for the piezo-phototronic effect.³² Our result is consistent with the previous theory and indicates that the efficiency enhancement is due to the polar piezo-phototronic effect. Moreover, although our device is demonstrated on a single NW, the same effect can be utilized to enhance the array LEDs using pattern or printing technique. Ultrasensitive and high resolution strain images may also be achieved through detection light variation from each NW LED under different strain.

In summary, we demonstrate a piezopotential tuned high efficiency ZnO NW/p-polymer air stable ultraviolet LED. The EQE of the hybrid LED can reach about 5.92%, which is comparable to that of inorganic p–n junction LED and quantum well-enhanced nanowire LED. Considering the difficulty in fabrication and conventional low efficiency in organic and inorganic/organic hybrid UV LED,^{17–23} this efficiency is a outstanding progress in reference to the published peer work. The significant enhancement is suggested due to a trimming of the electron current to match the hole current and increasing the localized hole density near the interface through the carrier channel induced by piezopotential. The asymmetric change of the I – V curve under negative and positive bias proves that the enhancement is due to the piezo-phototronic effect. The physical mechanism is explained by band diagram analysis and numerical simulation. The simulated trend of change in forward current under different strain is consistent with experimental results. Piezo-phototronic effect enhanced ZnO NW/p-polymer LED represents an interesting alternative to organic LEDs. Our devices possess the characteristics of high flexible and extremely high efficiency. The complete processing procedure is also compatible with large-area fabrication on flexible substrates. The approach pioneered in the study can be applied to other optoelectronic devices and may bring about significant performance improvement and energy saving.

ASSOCIATED CONTENT

Supporting Information

Experimental information, simulation details, and supporting figures and tables. This material is available free of charge via the Internet at <http://pubs.acs.org>.

AUTHOR INFORMATION

Corresponding Author

*E-mail: zhong.wang@mse.gatech.edu.

Author Contributions

||These authors contributed equally in this work.

Notes

The authors declare no competing financial interest.

ACKNOWLEDGMENTS

Research was supported by BES DOE (DE-FG02-07ER46394), NSF NSFC (61177062), and the Knowledge Innovation Program of the Chinese Academy of Sciences (KJCX2-YW-M13) and the Fundamental Research Funds for the Central Universities.

REFERENCES

- (1) Djurišić, A. B.; Ng, A. M. C.; Chen, X. Y. *Prog. Quant. Electron.* **2010**, *34*, 191.
- (2) Wang, Z. L.; Yang, R.; Zhou, J.; Qin, Y.; Xu, C.; Hu, Y.; Xu, S. *Mater. Sci. Eng. R* **2010**, *70*, 320.
- (3) Wang, Z. L. *Nano Today* **2010**, *5*, 540.
- (4) Heo, Y. W.; Norton, D. P.; Tien, L. C.; Kwon, Y.; Kang, B. S.; Ren, F.; Pearton, S. J.; LaRoche, J. R. *Mater. Sci. Eng. R* **2004**, *47*, 1.
- (5) Zimmler, M. A.; Capasso, F.; Müller, S.; Ronning, C. *Semicond. Sci. Technol.* **2010**, *25*, 024001.
- (6) Bao, J.; Zimmler, M. A.; Capasso, F.; Wang, X.; Ren, Z. F. *Nano Lett.* **2006**, *6*, 1719.
- (7) Park, W. I.; Yi, G.-C. *Adv. Mater.* **2004**, *16*, 87.
- (8) Zimmler, M. A.; Stichtenoth, D.; Ronning, C.; Yi, W.; Narayananamurti, V.; Voss, T.; Capasso, F. *Nano Lett.* **2008**, *8*, 1695.
- (9) Xu, S.; Xu, C.; Liu, Y.; Hu, Y.; Yang, R.; Yang, Q.; Ryou, J.-H.; Kim, H. J.; Lochner, Z.; Choi, S.; Dupuis, R.; Wang, Z. L. *Adv. Mater.* **2010**, *22*, 4749.
- (10) Weng, W.-Y.; Chang, S.-J.; Hsu, C.-L.; Chang, S.-P.; Hsueh, T.-J. *J. Electrochem. Soc.* **2010**, *157*, H866.
- (11) Soci, C.; Zhang, A.; Xiang, B.; Dayeh, S. A.; Aplin, D. P. R.; Park, J.; Bao, X. Y.; Lo, Y. H.; Wang, D. *Nano Lett.* **2007**, *7*, 1003.
- (12) Yang, Q.; Guo, X.; Wang, W.; Zhang, Y.; Xu, S.; Lien, D. H.; Wang, Z. L. *ACS Nano* **2010**, *4*, 6285.
- (13) Law, M.; Greene, L. E.; Johnson, J. C.; Saykally, R.; Yang, P. *Nat. Mater.* **2005**, *4*, 455.
- (14) Weintraub, B.; Wei, Y.; Wang, Z. L. *Angew. Chem., Int. Ed.* **2009**, *48*, 8981.
- (15) Sanchez, C.; Lebeau, B.; Chaput, F.; Boilot, J.-P. *Adv. Mater.* **2003**, *15*, 1969.
- (16) Nadarajah, A.; Word, R. C.; Meiss, J.; Könenkamp, R. *Nano Lett.* **2008**, *8*, 534.
- (17) Chang, C.-Y.; Tsao, F.-C.; Pan, C.-J.; Chi, G.-C.; Wang, H.-T.; Chen, J.-J.; Ren, F.; Norton, D. P.; Pearton, S. J.; Chen, K.-H.; Chen, L.-C. *Appl. Phys. Lett.* **2006**, *88*, 173503.
- (18) Könenkamp, R.; Word, R. C.; Godinez, M. *Nano Lett.* **2005**, *5*, 2005.
- (19) Na, J. H.; Kitamura, M.; Arita, M.; Arakawa, Y. *Appl. Phys. Lett.* **2009**, *95*, 253303.
- (20) Sun, X. W.; Huang, J. Z.; Wang, J. X.; Xu, Z. *Nano Lett.* **2008**, *8*, 1219.
- (21) Son, D. I.; You, C. H.; Kim, W. T.; Kim, T. W. *Nanotechnology* **2009**, *20*, 365206.
- (22) Zhao, S.-L.; Kan, P.-Z.; Xu, Z.; Kong, C.; Wang, D.-W.; Yan, Y.; Wang, Y.-S. *Org. Electron.* **2010**, *11*, 789.
- (23) Guo, H.; Zhou, J.; Lin, Z. *Electrochim. Commun.* **2008**, *10*, 146.
- (24) Guo, Z.; Zhang, H.; Zhao, D.; Liu, Y.; Yao, B.; Li, B.; Zhang, Z.; Shen, D. *Appl. Phys. Lett.* **2010**, *97*, 173508.
- (25) Braun, D.; Heeger, A. J.; Kroemer, H. *J. Electron. Mater.* **1991**, *20*, 945.
- (26) Benor, A.; Takizawa, S.-y.; Chen, P.; Pérez-Bolívar, C.; Anzenbacher, P. *Appl. Phys. Lett.* **2009**, *94*, 193301.
- (27) Yang, Q.; Wang, W.; Xu, S.; Wang, Z. L. *Nano Lett.* **2011**, *11*, 4012.
- (28) Pan, Z. W.; Dai, Z. R.; Wang, Z. L. *Science* **2001**, *291*, 1947.
- (29) Zhou, J.; Gu, Y.; Fei, P.; Mai, W.; Gao, Y.; Yang, R.; Bao, G.; Wang, Z. L. *Nano Lett.* **2008**, *8*, 3035.
- (30) Teke, A.; Özgür, Ü.; Doğan, S.; Gu, X.; Morkoç, H.; Nemeth, B.; Nause, J.; Everitt, H. O. *Phys. Rev. B* **2004**, *70*, 195207.
- (31) Zhang, B. P.; Binh, N. T.; Wakatsuki, K.; Segawa, Y.; Kashiwaba, Y.; Haga, K. *Nanotechnology* **2004**, *15*, S382.
- (32) Liu, Y.; Yang, Q.; Zhang, Y.; Yang, Z.; Wang, Z. L. *Adv. Mater.* **2012**, *24*, 1410.
- (33) Kim, K.-K.; Lee, S.-D.; Kim, H.; Park, J.-C.; Lee, S.-N.; Park, Y.; Park, S.-J.; Kim, S.-W. *Appl. Phys. Lett.* **2009**, *94*, 071118.
- (34) Bester, G.; Wu, X.; Vanderbilt, D.; Zunger, A. *Phys. Rev. Lett.* **2006**, *96*, 187602.
- (35) Hu, Y.; Zhang, Y.; Chang, Y.; Snyder, R. L.; Wang, Z. L. *ACS Nano* **2010**, *4*, 4220.
- (36) Sze, S. M. *Physics of Semiconductor Devices*; Wiley-Interscience: New York, 1981.